Soils and Rocks
An International Journal of Geotechnical and Geoenvironmental Engineering
www.soilsandrocks.com
ISSN 1980-9743
ISSN-e 2675-5475

Large-scale testing of free-ended piles in unsaturated expansive clays under cyclic and monotonic lateral loading

Ruan A. Murison[1#], Tiago A. V. Gaspar[2], Gerhard Heymann[1], Schalk W. Jacobsz[1], Ashraf S. Osman[3]

Article

Keywords
Pile foundations
Large-scale physical modelling
Field testing
Unsaturated expansive clays
Cyclic lateral loading

Abstract

This article presents an investigation into the influence of swell on the behaviour of large-scale free-ended piles installed in an unsaturated expansive clay deposit when subjected to lateral loading. A 'dry' pile was founded in a profile kept at natural water content conditions, and a 'wet' pile was founded in a profile which was flooded for six months to allow swelling of the clay prior to testing. Load cycles under two different load magnitudes were applied to the piles, followed by monotonic loading to failure. The applied load, pile head displacement and bending strain distributions with depth (determined using fibre Bragg gratings) were recorded during these tests. The behaviour under 113 kN load cycles was similar for the two piles, with the 'wet' pile exhibiting marginally stiffer response. This was attributed to a swell-induced increase in lateral stress acting against the pile shaft. Under load cycles of 145 kN and during the monotonic test, the 'wet' pile exhibited a substantially softer response and significantly lower ultimate capacity than that of the 'dry' pile. This was attributed to the effects of swell-induced softening and the reduced yield stresses in the swelled clay. These phenomena were interpreted with reference to a site investigation programme including seismic continuous surface wave tests and standard penetration tests, as well as some laboratory testing. Effects of local yielding of the bonded material at fissure interfaces upon pile ratcheting during cyclic loading have also been discussed.

1. Introduction

Expansive clays pose significant challenges for engineers worldwide. These clays are typically characterised by their high plasticity, causing them to significantly expand during wetting and shrink and crack during drying. This differential movement can have substantial economic consequences for overlying or adjacent structures (Jones & Holtz, 1973). The volumetric behaviour of such clays becomes a particular challenge in the context of wind turbines, where strict tolerances for differential foundation movements are typically prescribed.

Additionally, in the case of piled foundations, prior research has indicated that the aforementioned volume changes are accompanied by variations in shaft capacity (Blight, 1984; Elsharief et al., 2007; Gaspar et al., 2024). To address these challenges, the WindAfrica research project was initiated with the goal of developing practical guidelines for designing onshore wind turbine (piled) foundations in expansive soil conditions.

Previous publications on the WindAfrica project have presented (i) the hydromechanical behaviour of expansive clays (Gaspar et al., 2022; Murison et al., 2023), (ii) centrifuge modelling of piled foundations in expansive clays (Gaspar et al., 2024), and (iii) the response to soil swell of a large-scale instrumented pile socketed into bedrock (da Silva Burke et al., 2022). In the current study, the behaviour of large-scale free-ended piles under lateral loading is presented.

2. Background

Expansive soils are known to be a severe geohazard due to the distress imposed upon infrastructure by seasonal swelling and shrinkage. A number of construction techniques may be employed to mitigate these damages. Treatment or replacement of the expansive strata may be a feasible option, but is not recommended for depths beyond 2 m (Byrne et al., 2019). Another technique that may be employed to avoid excessive heaving of a foundation is pre-wetting

[#]Corresponding author. E-mail address: ruan.murison@tuks.co.za
[1]University of Pretoria, Department of Civil Engineering, Pretoria, South Africa.
[2]Imperial College, Department of Civil & Environmental Engineering, London, United Kingdom.
[3]Durham University, Department of Engineering, Durham, United Kingdom.

Submitted on January 31, 2025; Final Acceptance on July 31, 2025; Discussion open until February 28, 2026.
Editor: Renato P. Cunha
https://doi.org/10.28927/SR.2025.001925

the expansive profile and allowing swell to occur prior to construction, which is feasible up to depths of about 10 m (Weston, 1980; Byrne et al., 2019). If this method is implemented successfully and moisture loss of the layers is limited to avoid the effects of shrinkage, it is crucial to consider the influence of wetting the soil on the strength and resistance to deformation of the foundation system. Finally, the system may be isolated from the expansive layer using underreamed/anchored piles, as first suggested by Jennings & Henkel (1949). By providing anchorage at the base of the pile and a gap between the ground surface and the underside of a pile cap, this approach aims to provide a 'suspended' foundation. Although this is the most costly technique, the superstructure can be almost completely isolated from ground movements if the piles are sleeved (Fleming et al., 2009). If this technique is employed, thorough characterisation of the expansive soil is still required. Blight (1984) and Meintjes (1991) reported case studies where surface heave substantially exceeded what was predicted, causing the gap to swell shut and inducing heave-related damage to the superstructure. In cases where the bedrock or stable stratum is deep, this method might not be feasible. Expansive profiles extending to depths in the order of 30 m have been reported near Kimberley in South Africa (Byrne et al., 2019), and profiles in Sudan are commonly found to be deeper than 10 m (Elsharief, 2012). Under such conditions, founding the structure within the expansive strata may be the best option. In such cases, the use of piled foundations may be necessary to mitigate the effects of swell/shrink behaviour and may be particularly useful in cases where lateral loading is anticipated.

The design of pile foundations in expansive clays is a complex task due to the changes in lateral stress acting on the pile brought about by seasonal swelling and shrinkage of the clay, as well as the changes in resistance to lateral loading brought about by fluctuations in soil water content. The influence of these changes in moisture regime on the capacity of piles has been investigated in a handful of studies. Blight (1984) investigated the influence of wetting on shaft pull-out capacity for full-scale short piles. The shaft capacity increased by approximately 66% due to flooding of the profile for a 3 to 4-week period. Elsharief et al. (2007) reported a decrease in capacity of approximately 60% due to wetting for full-scale vertically loaded piles. In this case, the flooding had been maintained for two months. A study by Gaspar et al. (2024) shed light on these seemingly contradictory findings. In their study, centrifuge modelling was used to investigate the pull-out capacity of short piles, as well as the variation of lateral stresses acting on a long, wished-in-place pile instrumented with lateral load cells along its length. It was found that the lateral stresses acting on the pile increase initially during the swell process, and then reduce past initial 'pre-swell' values as the swelling process continues. It was thus suggested that an increase in capacity is exhibited early on into the swell process (or at low degrees of swell) due to the increase in lateral stresses on the pile, which was the mechanism observed by Blight (1984). At later stages of swell, a reduction in capacity is caused due to the effects of swell-induced softening, which was likely the mechanism observed by Elsharief et al. (2007). An effect of overburden stress upon the post-swelling capacity was also noted – the reduction in capacity at high degrees of swell was not prominent at greater depths where the clay swell (and thus swell-induced softening) was suppressed. Gaspar et al. (2024) thus concluded that the influence of swell on shaft capacity depends on the degree of swell, i.e. whether the increased lateral stress or the swell-induced softening is the dominant mechanism at the given stage of swell, as well as the given overburden stress.

The current study investigates the performance during lateral loading, under full-scale conditions.

3. Site investigation and in-situ testing

The large-scale testing described in this study took place adjacent to an existing bentonite mine near Vredefort, in the Free State Province of South Africa. A simplified borehole log, determined during site establishment, is presented in Figure 1a. Particle size distributions and soil classifications for samples taken from each of the distinct layers within the profile (at depths of 1.0, 3.0, and 5.0 m) are presented in Figure 1b and Table 1 respectively. X-ray diffraction (XRD) analyses confirmed that the dominant clay mineral constituent of each of the clays was smectite. This, along with the large plasticity indices and the highly fissured in-situ macrofabric, gives an indication of the high expansive potential of the profile.

Tests were conducted at two separate areas on the site. The first set of pile tests was conducted on a 'dry' area, where the soil was kept at natural water content conditions. A second set of tests (referred to as the 'wet' tests) was conducted on a section of the site which was flooded after pile installation for a period of six months. The flooding was facilitated using infiltration wells installed to a depth of 6 m. This allowed the intact masses within the fissured profile to swell prior to the pile testing. The two sections were sufficiently far apart (in excess of 50 m) to ensure that flooding of the 'wet' site did not influence the 'dry' site.

In-situ site characterisation tests were carried out at various stages throughout the project. The timeline of this testing, relative to the flooding period for the 'wet' site and the large-scale pile tests, has been summarised in Figure 2. Total rainfall over each complete wet and dry season within the monitoring period, which was recorded using a rain gauge installed at the site, has been included. Initial standard penetration tests (SPTs) were carried out at the eventual 'dry' and 'wet' site locations during site establishment, and no water table was observed at either location during this time. Approximately two months after site establishment, flooding of the 'wet' site commenced and continued for six months. Five weeks after the flooding period had been completed, the lateral pile loading tests commenced.

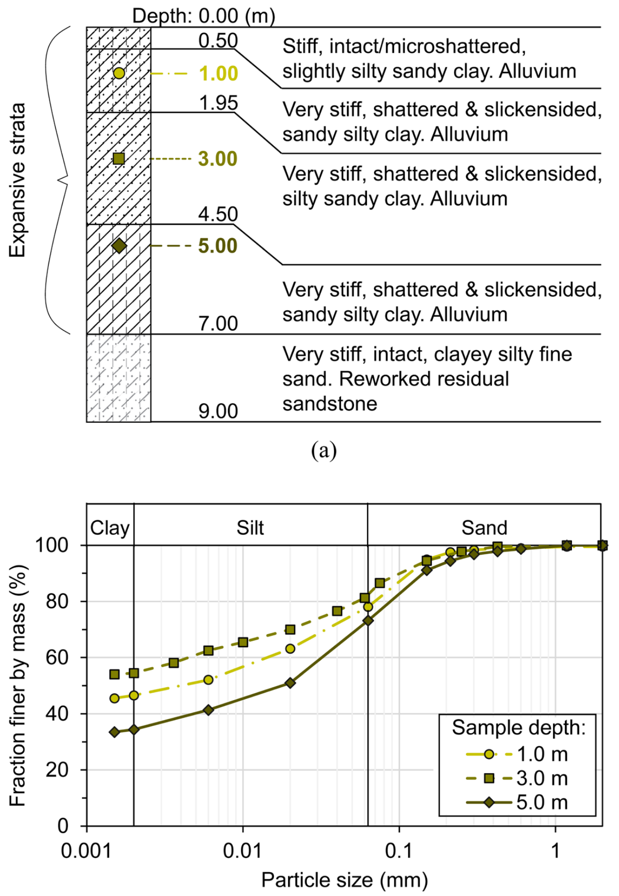

Figure 1. (a) Simplified soil profile from borehole logs; (b) particle size distributions at various sampling depths determined according to BS 1377-2 (BS, 1990).

This testing took place over a month-long period, during which the first sets of seismic continuous surface wave (CSW) tests were conducted as well. As a result of the flooding, the water table at the 'wet' site was observed to be very near the ground surface throughout the pile testing period. Throughout the subsequent 8-9 months, the upper strata of the 'wet' site profile partially dried out and the water table naturally subsided. At this stage, the second sets of SPT and CSW tests were conducted within two weeks of one another. The water table was observed at a depth of approximately 4 m during profiling of the 'wet' site, whilst the water table at the 'dry' site remained deep.

Table 1. Soil properties and classifications to BS 1377-2 (BS, 1990).

Property	Sample depth		
	1.0 m	3.0 m	5.0 m
In-situ water content, w (%) [a]	20.4	21.2	20.2
In-situ void ratio, e[a]	0.90	0.86	0.83
Specific gravity, G_s	2.662	2.692	2.669
Liquid limit, w_L (%)	66	109	72
Plasticity index, I_P (%)	47	82	50
Clay fraction by mass (%)	46	54	34
Classification (BS 1377-2)	CH	CE	CV
Smectite/illite-smectite content from XRD (%)	49	52	46
Activity (after Skempton, 1953)	1.02	1.52	1.39
Potential expansiveness class (after van der Merwe, 1975)	Very high	Very high	Very high

[a]At end of dry season.

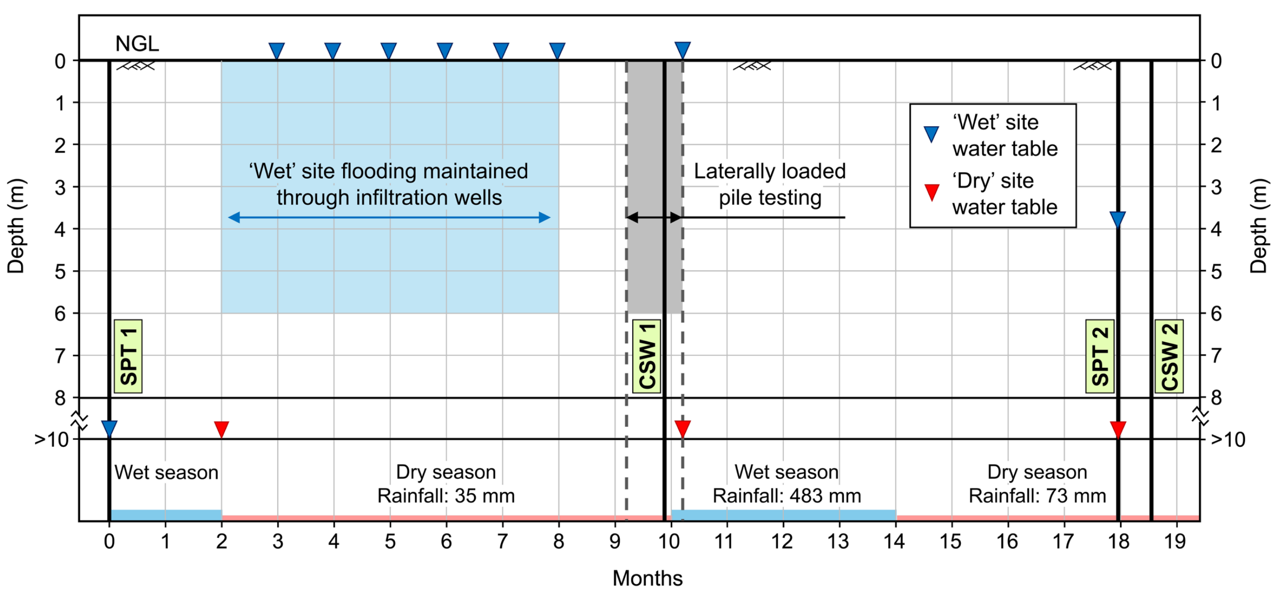

Figure 2. Timeline for flooding of the 'wet' site, in-situ testing and pile testing, along with respective water table positions and seasonal rainfall (after Murison et al., 2024).

The SPT blow counts were converted to equivalent N_{60} values (i.e. corresponding to the standard energy ratio of 60%), and are presented in Figures 3a and 3b. The profiles obtained during site establishment (i.e. prior to alteration of the water content of the 'wet' area) gave an indication of the uniformity of the site, and are given in Figure 3a. The profiles were satisfactorily similar for what would become the 'wet' and 'dry' sites. The second set of tests – conducted eight months after pile testing and after subsidence of the 'wet' site water table, given in Figure 3b – showed a significantly stiffer/stronger response at the 'dry' site, and a significantly softer/weaker response (at greater depth) at the 'wet' site. The initial profiles for each site are depicted using the broken lines in Figure 3b for reference. The changes in strength can be attributed to changes in suction occurring within the intact clay masses. As an example, gravimetric water contents for samples taken from a depth of 3 m at the site have varied naturally between approximately 27% after the wet season and 21% after the dry season. Soil-water retention curves for material from this depth showed that this variation would cause an increase in total suction from approximately 1.5 MPa to 6 MPa (Murison et al., 2023), which would induce a significant increase in shear strength and thus blow count. The first SPT tests were conducted in the middle of a wet season, and the second towards the end of a dry season. Such variations in water content would thus be expected, which explains the increase in blow count at the 'dry' site. The converse is also true: samples taken from the 'wet' site during the second set of SPT tests were approximately fully saturated at depths below 3.0 m, and a water table was established at 4.0 m. Suctions would thus be significantly lower at these depths, which would explain the reduction in blow count in the 'wet' site for depths below the water table.

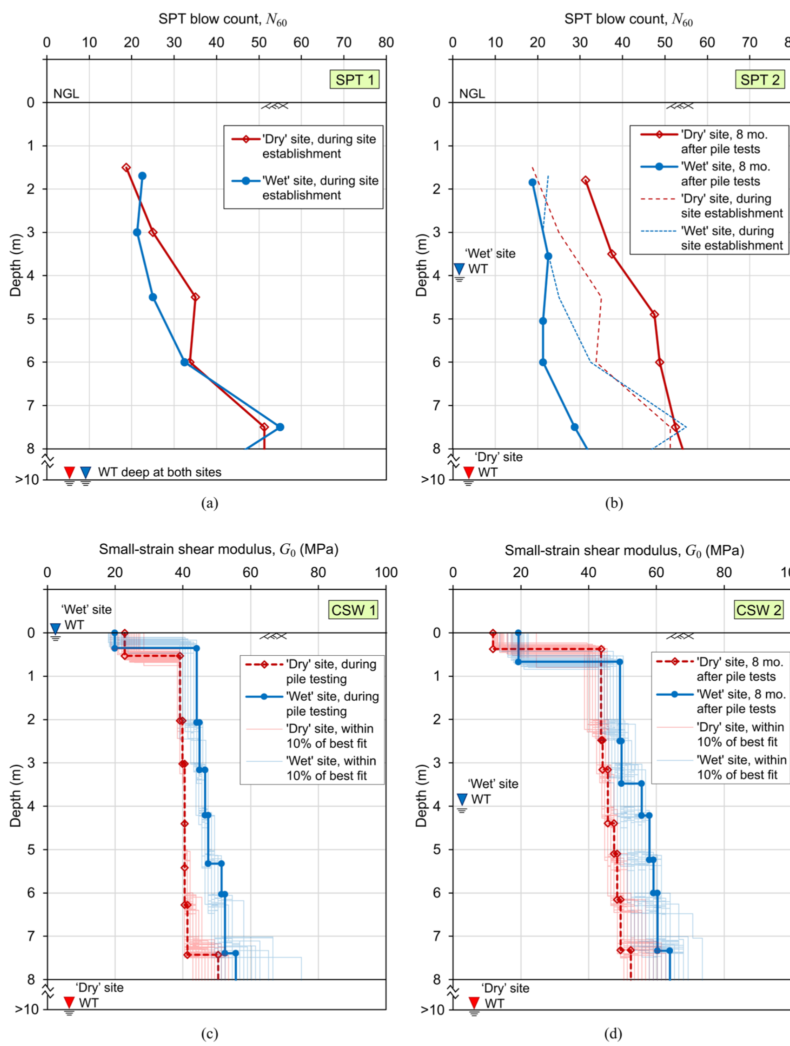

Figure 3. In-situ test results (after Murison et al., 2024): standard penetration test blow counts with depth for (a) SPT 1, conducted during site establishment, and (b) SPT 2, conducted 8 months after pile testing; small-strain shear modulus profiles with depth from seismic continuous surface wave tests for (c) CSW 1, conducted during pile testing, and (d) CSW 2, conducted 8 months after pile testing.

Detailed descriptions of the test setup and inversion algorithm used for the CSW testing and analyses were provided by Murison et al. (2024). The small-strain shear moduli (G_0) with depth resulting from the CSW testing and inversion are given in Figures 3c and 3d. All theoretical profiles trialled in the inversion search algorithm which contained a theoretical dispersion curve within 10% of the best-fit have also been reported in Figure 3. This gives an indication of the confidence level of the final profiles. At both instances in time and for both water table positions, the G_0 profiles for the two sites were similar. As a result, any engineering decisions for either site made on the basis of these measurements would not differ (this is supported by the overlap of the 10% misfits).

However, the 'wet' site profile was marginally stiffer in both cases. This observation is seemingly counterintuitive, as one would expect the stiffness of the 'wet' site profile to reduce during wetting due to the dissipation of suctions in the order of several megapascals, as discussed previously for the SPT results. The similarities may be explained by closer consideration of the fissured macrofabric of the clay profile and the strain range over which the measurement of shear moduli occurs during seismic tests. Matthews et al. (2000) reported significantly lower in-situ shear moduli for fissured hard soil and weak rocks using seismic techniques when compared to moduli measured in triaxial tests with local strain instrumentation. The very small strains imposed during CSW testing do not sufficiently deform the soil elements (within the intact masses) to close the fissures, and the measured shear wave velocity is thus dominated by the joint infill material rather than the intact material, which is tested in laboratory element tests. Regardless of whether or not wetting may have influenced the behaviour of intact material, if the fissures had not swelled closed and the fissure infill characteristics were not significantly changed, the measured small-strain stiffness would be similar. Additionally, if some of the fissures were to swell closed, the intact clay may start dominating the measured stiffness behaviour, and increases in the measured shear wave velocity (and thus G_0) would be expected.

4. Pile testing layout

The test layout was identical for both the 'dry' and 'wet' sites. The layout for the free-ended piles considered in this study is illustrated in Figure 4a. The setup consisted of two 600 mm diameter reinforced-concrete bored piles, at a 2 m centre-to-centre (c/c) spacing, embedded 6 m into the expansive clay profile.

Cyclic lateral loading was applied to the pile heads under load control using a hydraulic jack. The point of load application was 500 mm above the natural ground level (NGL). Lateral displacements of the piles during loading were measured using linear variable differential transformers (LVDTs) with a range of 50 mm, and the load applied through the hydraulic jack was recorded using a load cell with a 500 kN full-scale capacity. Fibre Bragg gratings (FBGs) were attached to the steel reinforcing to measure bending strain distributions along the length of the piles throughout testing. Detailed descriptions of the performance of these measurements relative to vibrating wire strain gauges – as well as the calculation procedure to obtain strains from the wavelengths recorded by the FBGs – were provided by Murison et al. (2022), who found that the tensile strain measurements using the different sensors were satisfactorily similar. Due to unforeseen circumstances, it was not possible to log the FBGs on the compression side of the piles for some of the tests considered in this study. Only tensile strain distributions (rather than bending moment distributions) have thus been

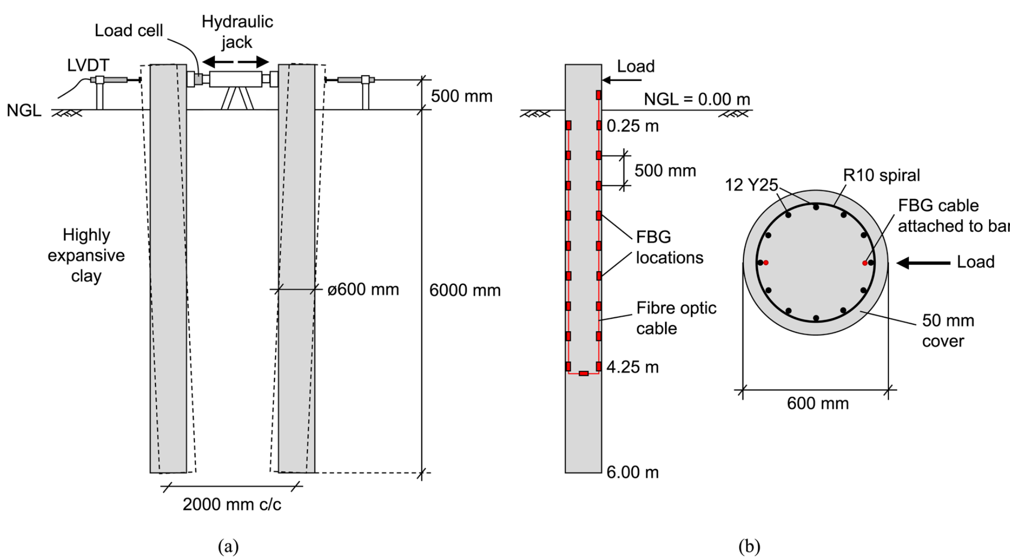

Figure 4. Experimental setup and instrumentation for lateral pile loading tests: (a) loading setup; (b) strain gauge layout and section details.

considered regarding bending behaviour. The positions of FBG sensors within the piles, as well as the reinforcement layout in the concrete section, are illustrated in Figure 4b. Note that the depiction of the fibre optic sensors is not to scale. The outer casing of the fibre optic cable was 1 mm in diameter, and each individual Bragg grating was 8 mm in length. Concrete testing was conducted on specimens cast on site and water-cured for 28 days. The properties of the concrete and steel reinforcement are summarised in Table 2.

The pile relative stiffness (K_R) was evaluated on the basis of Equation 1 (Poulos, 1982):

$$K_R = \frac{(EI)_{\text{pile}}}{E_{\text{soil}} L^4} \quad \begin{matrix} K_R > 0.2080 \text{ – rigid pile} \\ K_R < 0.0025 \text{ – slender pile} \end{matrix} \tag{1}$$

The Young's modulus of the soil (E_{soil}) at the pile base (L = 6 m) was estimated from the small-strain shear modulus determined in the CSW testing ($E_{soil} = 2(1+\nu)G_0$). Poisson's ratios of ν = 0.25 and ν = 0.5 were assumed for hypothetical drained and undrained loading respectively. As illustrated in Figure 3, the small-strain shear modulus at a depth of 6 m varied between approximately G_0 = 40 MPa and G_0 = 60 MPa. For drained loading, E_{soil} would thus vary between 100 and 150 MPa, resulting in a K_R range between 0.0011 and 0.0016. For undrained loading, E_{soil} would vary between 120 and 180 MPa, and K_R between 0.0009 and 0.0013. It is clear that regardless of the rate of loading imposed, the piles would be classified as slender according to the criterion set out in Equation 1.

5. Pile test results

The laterally loaded pile behaviour was evaluated based on the stiffness of the foundation system (i.e. lateral resistance), progressive displacement or "ratcheting" with increasing cycle number, and the bending strains experienced along the length of the pile at the peak of each cycle. The secant stiffness for each load–displacement cycle was calculated as illustrated in Figure 5, i.e. cycle stiffness was simply defined as the slope of a line connecting the trough and peak of a single load–displacement cycle. An initial set of 500 cycles under load control with a trough-to-peak load difference of approximately 100 kN and a maximum load of 113 kN was applied to the piles in the 'wet' and 'dry' sites. Thereafter, the maximum load magnitude was increased to approximately 145 kN for the 'wet' test for roughly 400 cycles. The pile considered in this study for the 'dry' test was not subjected to increased loading, but the first 400 cycles with a maximum load of 175 kN for an identical pile with identical loading history at the 'dry' site have been considered for comparison. Thereafter, the 'wet' and 'dry' piles considered initially were loaded monotonically to failure.

5.1 Initial cyclic loading

The maximum load for the initial load cycles was approximately 113 kN for both tests. The applied lateral load versus displacement for piles founded in clays under natural water content and swelled states are shown in Figures 6a and 6b respectively. The cycle stiffness versus cycle number is plotted for both piles in Figure 6c. Note that some portions of noisy data were caused by strong gusts of wind, which interfered with the LVDT measurements.

The 'dry' pile exhibited an accumulation of progressive displacement of approximately 0.5 mm over the 500 cycles. In addition, the cycle stiffness gradually increased with increasing cycle number, with an increase of approximately 14% from the start to end of loading. Given that the 'dry' test took place in a desiccated, highly fissured profile, this behaviour was attributed to local yielding of material along the fissure contacts. It is hypothesised that as the material at these contacts yielded, the displacement of the pile head

Table 2. Reinforced concrete material and section properties.

Property	Value	Test and/or reference
Steel Young's modulus (GPa)	200	Assumed for high-yield steel (BS, 2004)
Steel yield strength (MPa)	450	Assumed for high-yield steel (SABS, 2011)
Concrete Young's modulus (GPa)	27.8	E-value tests on 167 mm × ø150 mm cylinders (BS, 2021)
Concrete compressive cube strength (MPa)	34.9	Compression tests on 100 mm cubes (BS, 2019)
Concrete tensile strength (MPa)	2.0	Indirect tensile strength tests on 150 mm × ø150 mm split cylinders (BS, 2009)
Pile bending stiffness, $(EI)_{pile}$ (kNm)	$207.6 \cdot 10^3$	Section analysis, assuming uncracked pile

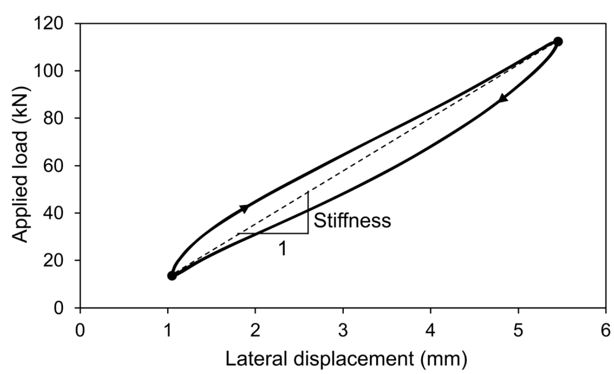

Figure 5. Definition of cycle stiffness for analyses.

progressively increased. However, as the process continued, the stiffer intact masses of clay would be pushed against each other at the fissure interfaces. As the behaviour of the system became increasingly dominated by the stiffness of the intact masses, the system cycle stiffness increased, and eventually tended to plateau around 500 cycles.

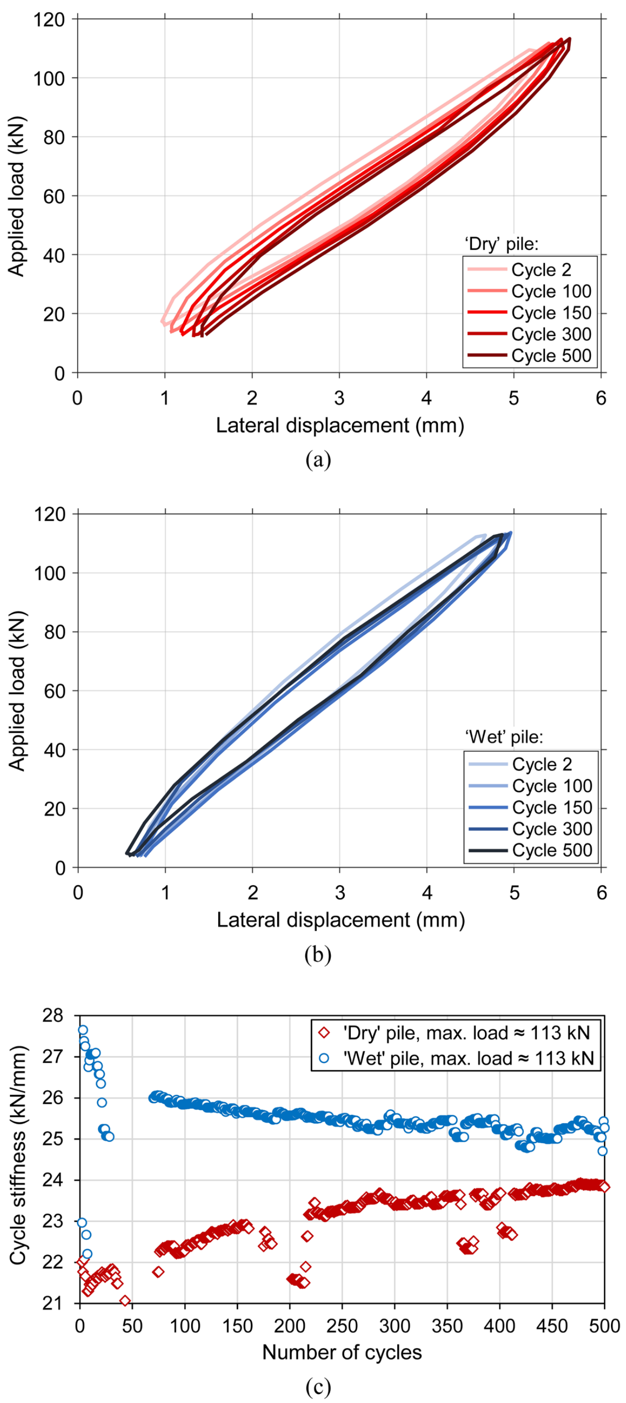

Figure 6. Cyclic test results for the initial 113 kN load cycles: (a) load vs displacement for 'dry' pile; (b) load vs displacement for 'wet' pile; (c) cycle stiffness for both piles.

Conversely, the 'wet' pile did not exhibit any significant ratcheting. Given that fissures would largely have swelled closed during the flooding process, local yielding within the infill material would not have occurred to the same extent during the subsequent application of lateral loading. Additionally, Gaspar & Jacobsz (2021) highlighted that as an initially unsaturated soil is wetted up, the strain required to cause failure (i.e. ductility) increases, which further justifies the absence of local yielding during the 'wet' test. It is noteworthy that the initial cycle stiffness for the 'wet' test was greater than that of the 'dry' test in Figure 6c. This is likely due to an increase in lateral net stress brought about due to the swelling of the clay, as was illustrated by the results reported by Gaspar et al. (2024). The increased confining stress would result in a decrease in volume compressibility of the clay, as long as the yield stress had not been exceeded. The stiffness of the 'wet' test system decreased marginally over the 500 cycles, with a total reduction of approximately 7%. The slight reductions can be described by considering the principles of unsaturated soil mechanics. Throughout the application of consecutive load cycles, local compaction would have occurred behind the pile. Assuming no changes in water content, this slight reduction in void ratio would have increased the degree of saturation, thus reducing the magnitude of soil suction and furthermore the stiffness of the clay. The same phenomenon was likely not observed for the 'dry' pile due to the high suction range under natural water content conditions, and the physical effects which dominate suction within this range. Monroy et al. (2015) performed oedometer tests with suction measurements, and found that expansive clay samples that were loaded or unloaded under constant water content conditions exhibited negligible changes in suction and vice versa, despite the volume changes invoked due to changes in net stress. These authors proposed that the relationship between water content and suction was unique (i.e. not influenced by volume change) beyond a certain suction threshold, due to the fact that suction is dominated by adsorption effects in this range (Baker & Frydman, 2009). This threshold was suggested to be between 100 and 400 kPa for various clay soils. As discussed previously, the suction at the 'dry' site would be at least an order of magnitude greater than this threshold based on measurements by Murison et al. (2023). Further evidence of a unique suction vs water content relationship at high suctions for the clay in this study was presented by Murison et al. (2023). Full primary drying and wetting curves were measured in the megapascal range for samples prepared at various different initial void ratios. Observable differences due to initial density could be seen in the suction vs void ratio and suction vs degree of saturation relationships, but there were no significant differences due to initial density in the suction vs water content relationships.

The bending strains measured along the length of the tension side of the piles at various cycle peaks have been plotted in Figure 7, where 1 με = 10^{-6} m/m. For both of the piles, there was no significant change in shape of the strain distribution with increasing cycle number. As shown in Figures 7a and 7b, any increase in the strain magnitude was largely confined to the first 100 cycles, after which the distributions remained constant for all practical purposes. For the gauges at depths between 0.75 m and 1.75 m (i.e. the three gauges that registered the largest strains for both piles), the increase in peak strain over the 500 cycles ranged between 6.3% and 9.9% for the 'dry' pile, and 11.2% and 14.6% for the 'wet' pile. Also illustrated in Figure 7 is the theoretical strain at which the concrete would crack (72 με), given the properties presented in Table 2 and assuming linear elastic behaviour prior to cracking. Evidently, cracking took place at the outermost fibres of the concrete section in the upper portions of both piles at the onset of load application. Figure 7c shows that whilst the strains in the 'dry' pile were of marginally greater magnitude, the bending behaviour of the 'wet' and 'dry' piles was notably similar. Maximum strains registered for the 'dry' and 'wet' piles were 280 με and 220 με respectively.

5.2 Cyclic loading under increased load magnitude

The lateral load–displacement responses for a 'dry' pile under cycles with a maximum load of 175 kN, and for the 'wet' pile under cycles with a maximum load of 145 kN, are given in Figures 8a and 8b respectively. The cycle stiffness behaviour for both cases is given in Figure 8c.

A contrast in behaviour is evident through the significant increase in magnitude of the displacements of the 'wet' pile in Figure 8b. The pile exhibited a significant reduction in stiffness immediately upon the application of the first load cycle, suggesting that the capacity of the system had been exceeded. Seeing as the same phenomenon did not occur for an identical reinforced-concrete pile at the 'dry' site, this reduced capacity has been attributed to the applied stresses under increased loading exceeding the yield stresses of the intact clay masses adjacent to the 'wet' pile. These yield stresses would have reduced due to swell-induced softening brought about during flooding of the 'wet' site (Gens & Alonso, 1992).

The 'dry' pile exhibited progressive displacement of approximately 1.8 mm, largely taking place within the first 100 cycles. After approximately 200 cycles, a stable load–displacement loop had formed with no further ratcheting. The 'wet' pile (which had not exhibited ratcheting under the 113 kN cycles) continued to accumulate progressive displacements throughout the 400 cycles, with a translation of more than 12 mm from the first to final cycle. In similar fashion to the previous load magnitude, as the cycle number increased the cycle stiffnesses marginally increased and decreased for the 'dry' and 'wet' piles respectively. These phenomena are likely to be attributable to the same respective mechanisms that were discussed for the 113 kN stages. One key difference is that the 'dry' pile cycle stiffness was roughly equal for the final cycle under both load magnitudes, whereas the 'wet' pile exhibited a reduction in cycle stiffness in excess of 80% due to an increase in load magnitude of approximately 28%.

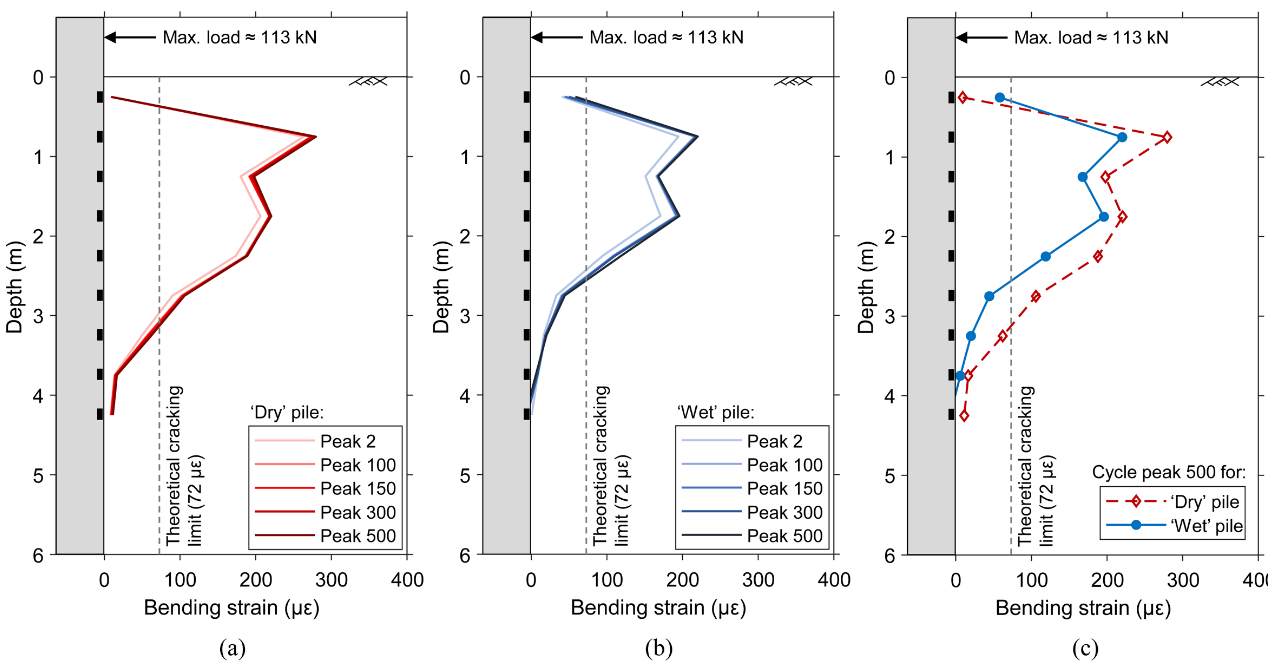

Figure 7. Bending strain distributions measured on the tension side of the piles at cycle peaks under the initial 113 kN load cycles: (a) 'dry' pile; (b) 'wet' pile; (c) comparison of final cycles.

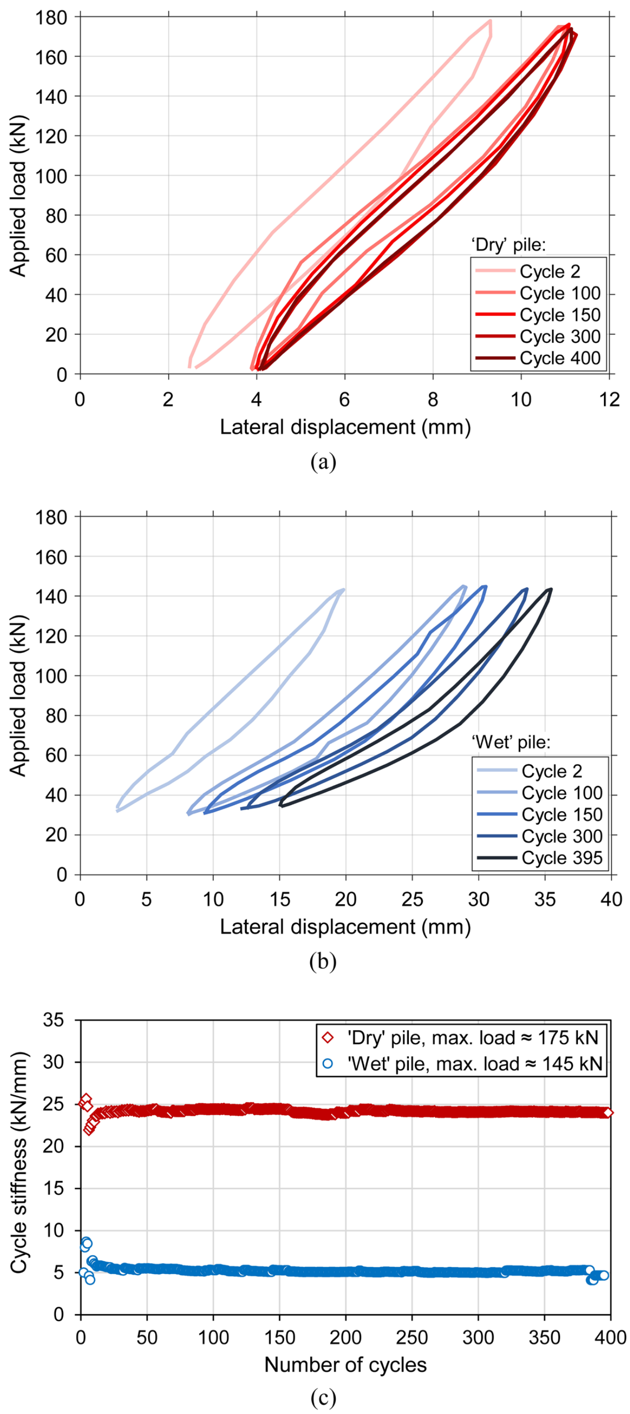

Figure 8. Cyclic test results under increased load magnitudes: (a) load vs displacement for 'dry' pile; (b) load vs displacement for 'wet' pile; (c) cycle stiffness for both piles. Note the different displacement axis scales.

The distributions of tensile strain due to bending for various cycle peaks are given in Figure 9. Once more, it should be noted that the 'dry' pile considered here is not the same pile considered in the previous and subsequent sections, but rather an identical pile founded in the 'dry' site with identical loading history prior to this test. This is the reason for the slightly different shape in bending strain distribution when comparing Figures 7a and 9a. A significant crack had developed in the 'dry' pile at the onset of loading, with a maximum strain of 795 με at 1.25 m. The greatest change in strain registered over the application of 400 load cycles was at 2.25 m, where the progression of cracking caused an increase in strain of 39% (from 184-256 με), the majority of which took place during the first 100 cycles. However, the shape and magnitude of the strain distribution remained largely unchanged under repeated loading. The 'wet' pile exhibited strains exceeding 400 με over the entire upper 4 m of the pile from the onset of loading. This indicates significant cracking throughout the pile due to the reduced post-yielding soil resistance. The cracks continued to propagate as further load cycles were applied, with a tensile strain increase between 36 and 43% in the first 100 cycles and an increase between 52 and 67% over the entire 395 cycles (considering depths between 0.75 m and 3.75 m). The maximum strain experienced at these higher applied loads (1347 με at 1.75 m) was 512% greater than that of the previous load stage, despite an increase in load of only 28%, highlighting the severe contrast in behaviour after the intact clay masses had yielded. Considering the properties outlined in Table 2 and assuming linear elastic conditions for steel, the steel reinforcement to which the FBGs were attached would yield at 2250 με, which would constitute ultimate failure of the pile. Since the strains did not exceed this limit, the pile at the 'wet' site had not structurally failed during this test, but displacement of over 35 mm would constitute a serviceability failure for many applications.

Although the increase in lateral stress due to swelling of the clay increased the system stiffness at lower imposed loads, the effects of swell-induced softening were evident under the increased load. This was marked by a reduction in both the resistance (cycle stiffness) and the serviceable capacity of the 'wet' pile when compared to the 'dry' pile. It is thus likely, with reference to the discussion by Gaspar et al. (2024), that the degree of swell at the time of testing was such that the dominant mechanism influencing pile capacity was swell-induced softening.

5.3 Monotonic loading to failure

After the application of load cycles, the piles were loaded monotonically to 'failure' under load control. During these tests, the monotonic load was incrementally ramped up and held constant for a period of 10 minutes at each target load. Due to the large deformations anticipated for the 'wet' pile, an LVDT with a range of 100 mm was used. After the loading phase was complete, the load was incrementally reduced back to zero whilst the unloading displacements were recorded. Figure 10a shows the applied load versus lateral displacement for the 'dry' and 'wet' piles. Figure 10b shows the secant stiffness relative to the origin (i.e. the ratio between load and displacement at any point) for the monotonic tests.

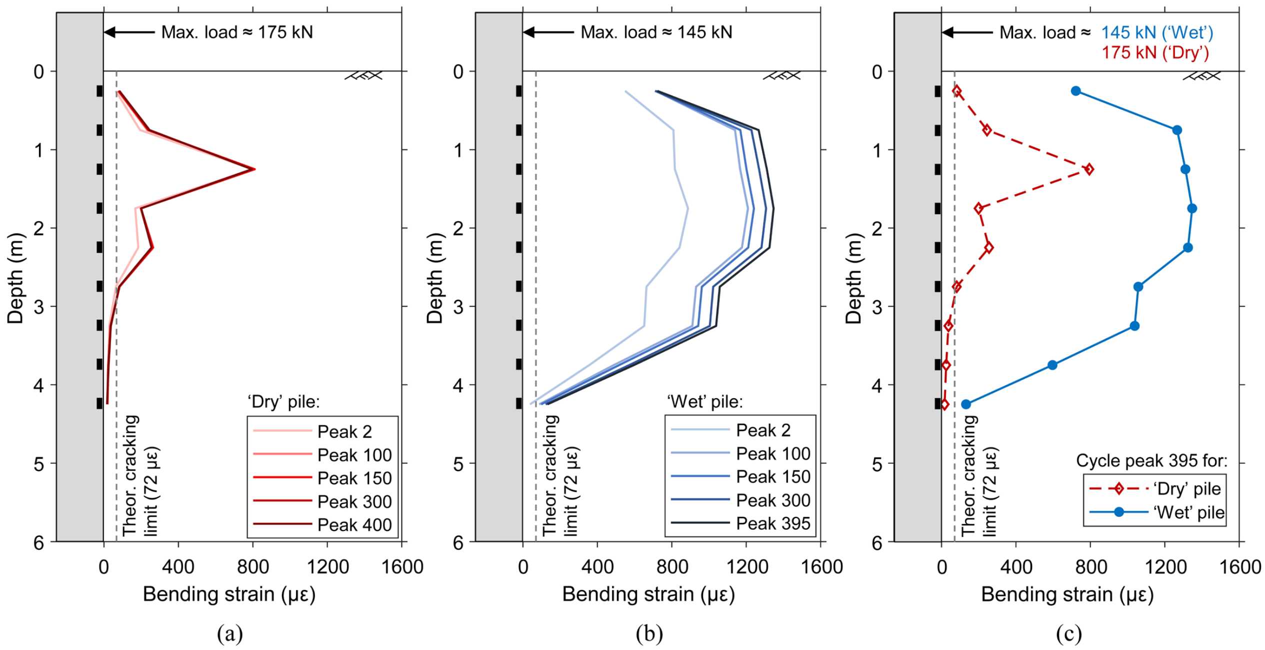

Figure 9. Bending strain distributions measured on the tension side of the piles at cycle peaks under increased load magnitudes: (a) 'dry' pile; (b) 'wet' pile; (c) comparison of final cycles.

To reference the cyclic test results to the monotonic tests, the cycle stiffness ranges for each peak load magnitude have been included in Figure 10b as well.

In contrast to the cyclic tests, the 'dry' pile exhibited a stiffer response than the 'wet' pile from the onset of loading. This is most likely due to the significant cracking and associated reduction in structural stiffness of the 'wet' pile that occurred during the second cyclic stage. Once the loads applied during the cyclic test stages had been exceeded, the 'dry' pile continued to exhibit a stiffer response than that of the 'wet' pile by at least a factor of two for all load magnitudes. At the maximum applied load of 413 kN for the 'dry' test, the maximum pile head displacement was 27.0 mm (4.5% of the pile diameter). For the 'wet' test, upon reaching a maximum load of 366 kN, the actuator went out of range, causing a reduction in load from 366 to 316 kN over the period where the load was meant to be held constant. However, despite the decrease in applied force, the lateral displacement continued to increase. This indicated ultimate structural failure of the pile (a fact that is supported by the later discussion of measured strain distributions). A maximum displacement of 68.4 mm (11.4% of the pile diameter) was recorded for the 'wet' test. After unloading back to a lateral load of 0 kN, 4.8 mm and 12.9 mm of imposed permanent deformation were recorded for the 'dry' and 'wet' piles respectively.

The distributions of tensile strain due to bending at the start and end of various target loads are given in Figure 11. Upon inspection of the 'wet' test distributions in Figure 11b, ultimate structural failure of the pile can be confirmed seeing as strains which significantly exceed the limit at which steel

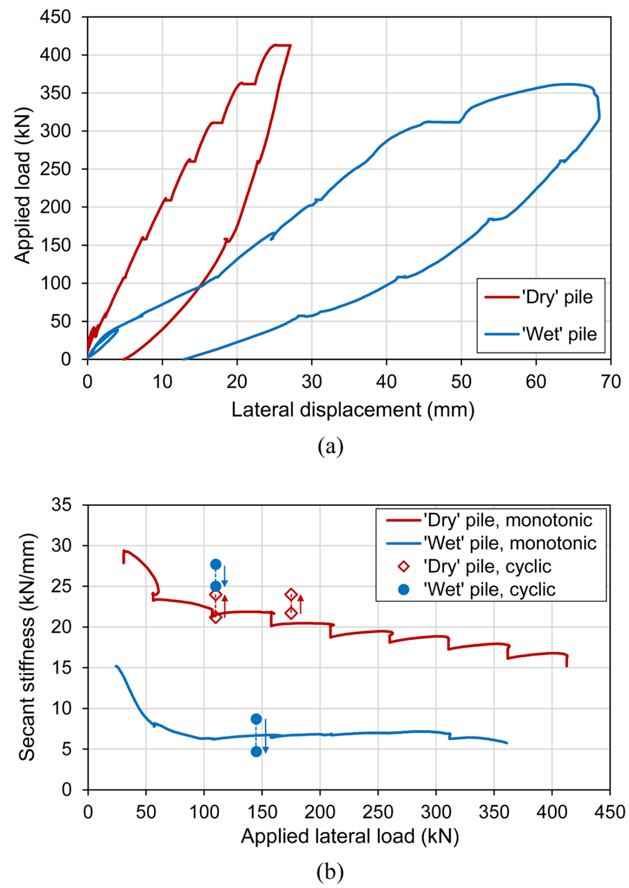

Figure 10. Monotonic test results: (a) load–displacement behaviour under monotonic loading and unloading; (b) secant stiffness as a function of peak lateral load for the monotonic and cyclic tests.

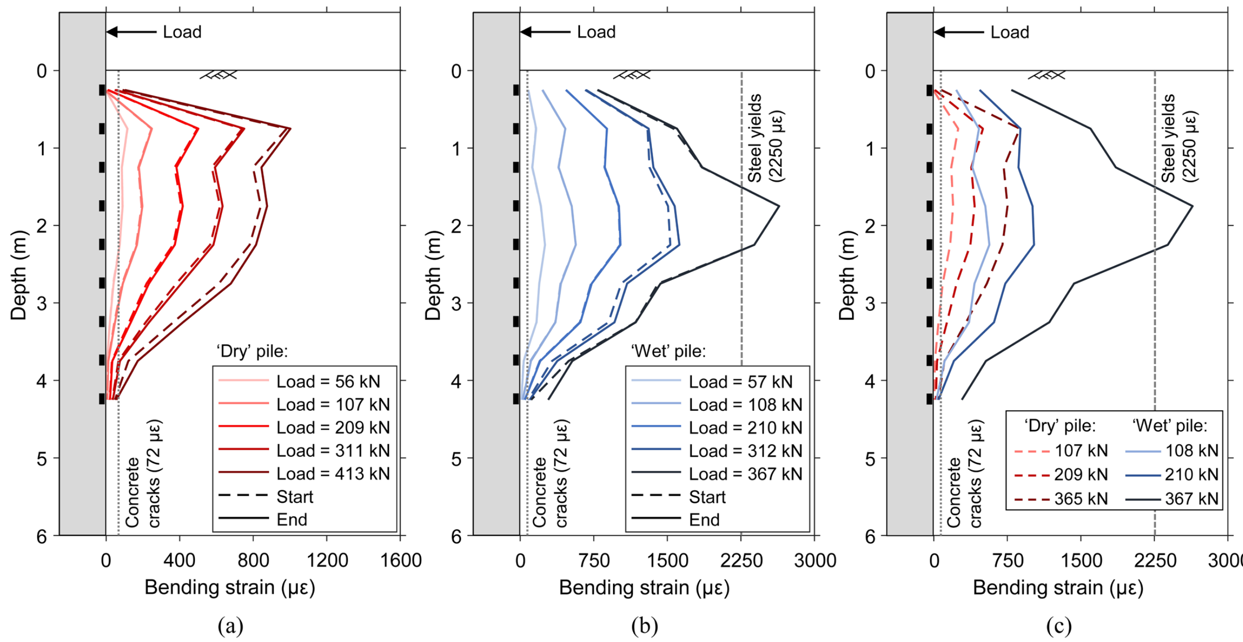

Figure 11. Bending strain distributions measured on the tension side of the piles at various load magnitudes during monotonic loading: (a) 'dry' pile; (b) 'wet' pile; (c) comparison of final cycles. Note the different strain axis scale for (a).

yields were recorded at depths of 1.75 m and 2.25 m. The shape of the strain distribution for the 'dry' pile in Figure 11a closely resembled the shape exhibited in the 113 kN cyclic stage (Figure 7a). A maximum strain of 1002 με was recorded at the maximum load of 413 kN. Despite the maximum load being nearly 3 times greater, the largest bending strain and pile head displacement recorded during the monotonic 'dry' test were both less than that of the 145 kN cyclic stage for the 'wet' pile. Considering the comparison presented in Figure 11c, it is also evident that the bending strains of the 'wet' pile were substantially greater than those of the 'dry' pile at all depths during monotonic loading. These observations all highlight the considerable contrast in behaviour of piles in the large-strain (i.e. high stress) range that is brought about by swelling of the expansive clay.

The effects of the structural damage incurred by the 'wet' pile during the 145 kN cyclic stage can be further illustrated by considering the strain distributions registered during the 113 kN cyclic stages, compared with the distributions at the same load magnitude during the monotonic tests. These have been illustrated for both piles in Figure 12. The distributions after 500 cycles at 113 kN are given by the broken lines. Due to the permanent deformations from the 145 kN cyclic stage, when reloaded to 108 kN monotonically, the 'wet' pile exhibited strains more than double that of the 113 kN cyclic stage for depths up to 2.25 m, and an order of magnitude greater from 2.75 m onwards. The presence of these permanent strains gives an indication of the permanent bending moments built into the 'wet' pile after cyclic loading. In contrast, the 'dry' pile strains when reloaded to 107 kN closely resembled the strains at the end of the 113 kN cyclic loading stage. In fact, the monotonic test strains were slightly lower than those recorded during cyclic loading, likely due to the 6 kN difference in load magnitude.

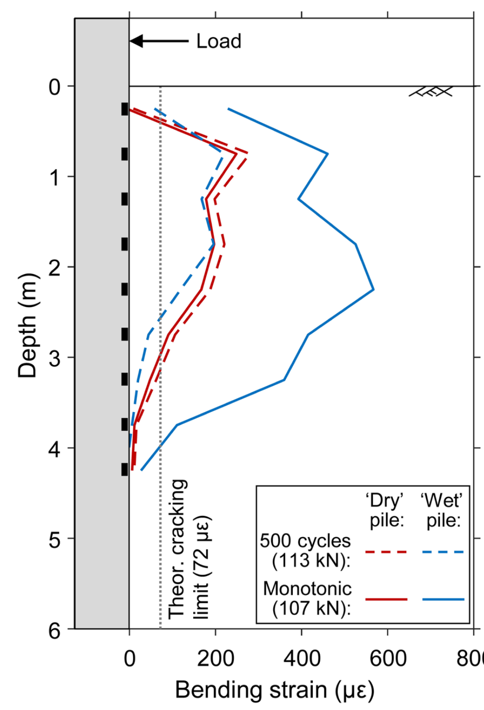

Figure 12. Bending strain distributions measured on the tension side of the piles at approximately 110 kN, for the 500th cycle during initial cyclic loading and for the monotonic loading after the cyclic tests.

The differences in behaviour depending on moisture conditions and stress levels, as well as the associated implications, have been summarised with reference to the site characterisation data and element tests in the following section.

6. Insights from in-situ and laboratory tests

The results presented in this study have highlighted that the behaviour of piles under different moisture conditions highly depends on the range of strains or stresses to which they are subjected. To extend the conclusions reached by Gaspar et al. (2024): whether swelling of an expansive clay causes an increase or decrease in resistance to lateral pile deformation is not only a function of the degree of swell and overburden stress, but also of the magnitude of lateral loading being imposed on the soil. At the initial stress range tested, piles founded in expansive clay that had been artificially flooded for six months to induce swell exhibited marginally stiffer mechanical responses to piles founded in the same expansive clay profile at natural water content conditions after the dry season. This was attributed to an increase in lateral stress acting on the pile due to the clay swell. However, at higher applied loads (and thus strains), the mechanical response of the 'wet' pile in the artificially swelled clay was substantially softer than that of the 'dry' pile in clay under natural moisture conditions, as indicated by far larger displacements and bending strains. Under increased loading, it became evident that although the lateral stress had increased due to swell, the effects of swell-induced softening were the dominant mechanism. These trends were reflected in the in-situ test results as well. The shear moduli determined at very small strains from CSW testing were similar at the 'wet' and 'dry' sites (with slightly higher stiffnesses for the 'wet' site), but the large-strain penetration resistance (from SPTs) of the 'wet' site was substantially lower than that of the 'dry' site.

It was suggested that the differences in observed pile behaviour were due to the fact that the yield stress of the intact masses of soil in which the 'wet' pile was founded had been exceeded. The soil in which the 'dry' pile was founded had not yielded despite being tested at the same load magnitude. This can be explained by considering the phenomenon of swell-induced softening. Gens & Alonso (1992) illustrated the concept through a critical state soil mechanics-based constitutive model for highly expansive unsaturated clays. The model allows for a reduction in macrostructural yield stress to be induced by the microstructural swelling that occurs due to the reduction in suction along a wetting path. This reduction in yield stress was evident in a double oedometer test conducted on samples obtained at the test site in the current study from a depth of 3 m. The test was conducted according to guidelines by Jennings & Knight (1957), and is depicted in Figure 13. Note that the stress state variable used is net vertical stress ($\bar{\sigma}_v$), which is simply vertical total stress minus pore air pressure (which is assumed to be equal to zero). Figure 13a shows the incremental loading path of a sealed sample under constant water content (emulating 'dry' site conditions), as well as a parallel sample where the cell was flooded under a seating stress of 50 kPa (the approximate in-situ net vertical stress at 3 m) and allowed to swell (thus emulating 'wet' site conditions). Casagrande (1936) constructions were used to determine the yield stress ($\bar{\sigma}_{v,y}$) for each sample. The yield stress for the sample that was soaked and brought to zero suction was approximately an order of magnitude lower than that of the sample loaded at natural water content. The stiffness of the samples at various stress ranges has been expressed through constrained modulus ($E_{oed} = \Delta\bar{\sigma}_v / \Delta\varepsilon_v$, where ε_v is volumetric strain). The constrained modulus for each test has been normalised by net stress in Figure 13b. This aims to separate the reduction in stiffness due to yielding from the increases in stiffness due to increasing confining stress. This figure shows the drastic reduction in stiffness after yielding of the 'wet' sample, and shows the significant difference in stiffness behaviour between

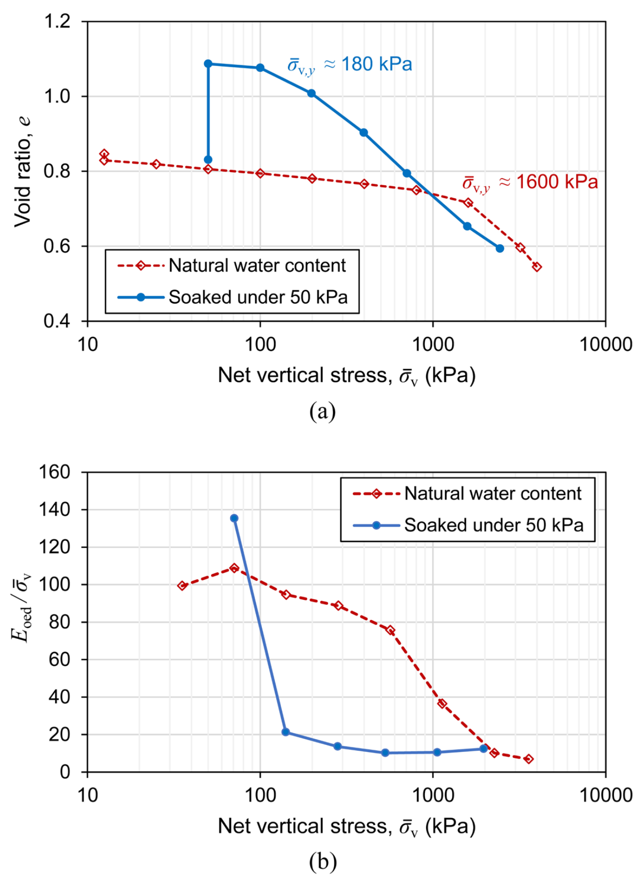

Figure 13. Double oedometer test results showing (a) reduction in yield stress due to swell, and (b) differences in soil stiffness due to swell.

the ‘wet’ and ‘dry’ samples at stresses greater than the ‘wet’ yield stress and less than the ‘dry’ yield stress. This region is an analogy for the loading range within which the ‘wet’ and ‘dry’ piles exhibited substantially different behaviour. Interestingly, the constrained modulus for the ‘wet’ sample prior to yielding was similar in magnitude (and marginally greater) than that of the ‘dry’ sample. This mimics the trend observed in the CSW G_0 profiles and in the initial pile response under the 113 kN cycles.

Although it may be straightforward to understand and categorise the pile response into small-strain and large-strain (or pre-yielding and post-yielding) behaviour, the primary challenge in implementing these findings would be determining the load at which this distinction occurs for a pile founded in expansive clay that has been subjected to large changes in water content. An increase in lateral load of 28% from 113 kN to 145 kN resulted in a five-fold reduction in secant stiffness response and a five-fold increase in maximum tensile strain from bending for the ‘wet’ pile.

It is thus imperative when designing piles in expansive clays for lateral loading to carefully consider the interrelationship of three factors and the influence that these may have on the functional capacity: (i) the duration of swelling expected, along with the ground conditions, drainage boundaries and permissible temporal water content fluctuations that may occur in situ, (ii) the changes in yield stress that these fluctuations might bring about through swell-induced softening, and (iii) the expected magnitude of loading and whether this might cause exceedance of these yield stresses of the intact swelled soil, leading to a transition from small-strain to large-strain pile behaviour.

7. Conclusions

This study detailed an investigation into the effects of clay swell on the lateral resistance of large-scale free-ended piles by comparing behaviour of a ‘dry’ pile founded in expansive clay under natural water content conditions to that of a ‘wet’ pile, which was founded in the same clay but subjected to a six-month wetting period. Under the application of 500 cycles with a maximum load of 113 kN, the two piles exhibited similar behaviour in terms of load–displacement response, cycle secant stiffness and bending strains. The ‘wet’ pile exhibited a marginally greater resistance to deformation in this test, which was attributed to the increase in lateral stress against the pile shaft due to swelling of the clay. When the magnitude of the maximum load was increased to 145 kN for the ‘wet’ pile and 175 kN for a ‘dry’ pile for the subsequent 400 cycles, no substantial change in behaviour was evident for the ‘dry’ pile, but a severe reduction in stiffness and the onset of large displacements and bending strains were noted for the ‘wet’ pile. This was attributed to the effects of swell-induced softening, which had significantly reduced the yield stress of the intact clay masses within which the pile was founded. A five-fold increase in bending strains and five-fold reduction in cycle stiffness were brought about by a 28% increase in lateral load, which highlighted the clear contrast in pre-yielding and post-yielding behaviour of the swelled clay. Monotonic load tests aimed at causing failure of the piles were conducted after cyclic loading. A maximum load of 413 kN was applied to the ‘dry’ pile, at which point the secant stiffness remained twice that of the ‘wet’ pile after the 145 kN cyclic stage. Additionally, the maximum bending strains were significantly lower in magnitude than those of the 145 kN ‘wet’ pile cyclic stage. No signs of structural failure were observable for the ‘dry’ pile. The ‘wet’ pile exhibited a softer response than that of the ‘dry’ pile throughout monotonic loading and reached ultimate structural failure at a load of 366 kN. At ultimate failure, the tensile strains had exceeded the steel reinforcement yielding limit and a maximum displacement of 68.4 mm (0.114 times the pile diameter) was registered.

Gaspar et al. (2024) concluded that two mechanisms may influence pile capacity during swelling of an expansive clay. An increase in capacity may be brought about by a swell-induced increase in lateral stress, and a decrease in capacity by the effects of swell-induced softening. The dominant mechanism was found to be strongly dependent on the degree of swell, which can vary both temporally and spatially throughout a clay profile. In the current study, it was observed that the magnitude of strain imposed by applied loading may also influence which mechanism dominates pile behaviour. At lower load levels, the pile in swelled clay exhibited greater stiffness, consistent with an increase in lateral stress. However, at higher load magnitudes, where larger strains developed, swell-induced softening became the dominant mechanism. This resulted in a significantly softer response and reduced serviceable and ultimate capacities against lateral loading.

Acknowledgements

The authors would like to express their gratitude to the UK Engineering and Physical Sciences Research Council (EPSRC) Global Challenges Fund for the financial support under the WindAfrica project, Grant Ref: EP/P029434/1. The authors would also like to thank Dr Gerrit Smit from the University of Pretoria who supervised large portions of the pile installations for this study, and Dr Hendrik Louw from the University of Pretoria who conducted the concrete material property tests.

Declaration of interest

The authors have no conflicts of interest to declare. All co-authors have observed and affirmed the contents of the paper and there is no financial interest to report.

Authors' contributions

Ruan A. Murison: conceptualization, formal analysis, investigation, methodology, visualisation, writing – original draft. Tiago A. V. Gaspar: conceptualization, methodology, visualisation, supervision, writing – review and editing. Gerhard Heymann: conceptualization, formal analysis, supervision, writing – review and editing. Schalk W. Jacobsz: conceptualization, funding acquisition, project administration, supervision, writing – review and editing. Ashraf S. Osman: conceptualization, funding acquisition, project administration, writing – review and editing.

Data availability

The data generated and analysed in this study are available from the corresponding author by request.

Declaration of use of generative artificial intelligence

This work was prepared without the assistance of any generative artificial intelligence (GenAI) tools or services. All aspects of the manuscript were developed solely by the authors, who take full responsibility for the content of this publication.

List of symbols and abbreviations

e	void ratio
$(EI)_{\text{pile}}$	bending stiffness of the pile
E_{oed}	constrained modulus
E_{soil}	Young's modulus of the soil at the pile base
G_0	small-strain shear modulus
G_s	specific gravity
I_P	plasticity index
K_{R}	relative stiffness of the pile
L	pile embedment depth
N_{60}	SPT blow count at standard energy ratio of 60%
w	gravimetric water content
w_L	liquid limit
$\Delta\varepsilon_{\text{v}}$	change in volumetric strain
$\Delta\bar{\sigma}_{\text{v}}$	change in net vertical stress
ε_{v}	volumetric strain
ν	Poisson's ratio
$\bar{\sigma}_{\text{v}}$	net vertical stress
$\bar{\sigma}_{\text{v},y}$	net vertical yield stress
c/c	centre-to-centre
CSW	continuous surface wave
FBG	fibre Bragg grating
LVDT	linear variable differential transformer
NGL	natural ground level
SPT	standard penetration test
WT	water table
XRD	X-ray diffraction

References

Baker, R., & Frydman, S. (2009). Unsaturated soil mechanics: critical review of physical foundations. *Engineering Geology*, 106(1-2), 26-39. http://doi.org/10.1016/j.enggeo.2009.02.010.

Blight, G.E. (1984). Power station foundations in deep expansive soil. In *Proceedings of the 1st International Conference on Case Histories in Geotechnical Engineering* (Vol. 1, pp. 77-86), St. Louis, Missouri. University of Science and Technology.

BS 1377-2:1990. (1990). *Methods of test for soils for civil engineering purposes – part 2: classification tests*. British Standards Institution, London.

BS EN 1992-1:2004. (2004). *Eurocode 2: design of concrete structures*. British Standards Institution, London.

BS EN 12390-6:2009. (2009). *Testing hardened concrete: tensile splitting strength of test specimens*. British Standards Institution, London.

BS 12390-3. (2019). *Testing hardened concrete: compressive strength of test specimens.* British Standards Institution, London.

BS EN 12390-13:2021. (2021). *Testing hardened concrete: determination of secant modulus of elasticity in compression*. British Standards Institution, London.

Byrne, G., Chang, N. & Raju, V. (2019). *A guide to practical geotechnical engineering in Africa* (5th ed.). Johannesburg: Franki, A Keller Company.

Casagrande, A. (1936). The determination of the pre-consolidation load and its practical significance. In *Proceedings of the 1st International Conference on Soil Mechanics and Foundation Engineering* (Vol. 3, pp. 60-64), Cambridge, MA. Winchester: Geomechanical Engineers Inc.

da Silva Burke, T.S., Jacobsz, S.W., Elshafie, M.Z.E.B., & Osman, A.S. (2022). Measurement of pile uplift forces due to soil heave in expansive clays. *Canadian Geotechnical Journal*, 59(12), 2119-2134. http://doi.org/10.1139/cgj-2021-0079.

Elsharief, A.M. (2012). Foundations on expansive soils, Sudan experience. In *Proceedings of the Graduate School Conference, on Basic Sciences and Engineering*. Khartoum: University of Khartoum.

Elsharief, A.M., Ahmed, E.O., & Mohamedzein, Y.E.A. (2007). Guidelines for the design of bored concrete piles in expansive soils of Sudan. In *Proceedings of the Graduate School Conference, on Basic Sciences and Engineering*. Khartoum: University of Khartoum.

Fleming, W.G.K., Weltman, A., Randolph, M.F., & Elson, W.K. (2009). *Piling engineering* (3rd ed.). London: Taylor & Francis.

Gaspar, T.A.V., & Jacobsz, S.W. (2021). Brazilian Tensile Strength Test conducted on ductile unsaturated soil samples. *Geotechnical Testing Journal*, 44(3), 799-810. http://doi.org/10.1520/GTJ20190078.

Gaspar, T.A.V., Jacobsz, S.W., Heymann, G., Toll, D.G., Gens, A., & Osman, A.S. (2022). The mechanical properties of a high plasticity expansive clay. *Engineering Geology*, 303, 106647. http://doi.org/10.1016/j.enggeo.2022.106647.

Gaspar, T.A.V., Jacobsz, S.W., Smit, G., & Osman, A.S. (2024). Centrifuge modelling of piled foundations in swelling clays. *Canadian Geotechnical Journal*, 61(1), 46-58. http://doi.org/10.1139/cgj-2022-0449.

Gens, A., & Alonso, E.E. (1992). A framework for the behaviour of unsaturated expansive clays. *Canadian Geotechnical Journal*, 29(6), 1013-1032. http://doi.org/10.1139/t92-120.

Jennings, J.E.B. & Henkel, D.J. (1949). *The use of under-reamed pile foundations on expansive clay soils in South Africa* (CSIR NBRI Report BRR, No. 32). CSIR-National Building Research Institute.

Jennings, J.E.B., & Knight, K. (1957). The prediction of total heave from the double oedometer test. *Transactions of the South African Institution of Civil Engineers*, 7(9), 285-291.

Jones, D.E., & Holtz, W.G. (1973). Expansive soils: the hidden disaster. *ASCE Civil Engineering*, 43(8), 49-51.

Matthews, M.C., Clayton, C.R.I., & Own, Y. (2000). The use of field geophysical techniques to determine geotechnical stiffness parameters. *Geotechnical Engineering*, 143(1), 31-42. http://doi.org/10.1680/geng.2000.143.1.31.

Meintjes, H.A.C. (1991). A case history on heaving clay: Colinda Primary School. In: G.E. Blight, A.B. Fourie, I. Luker, D.J. Mouton & R.J. Scheurenberg (Eds.), *Geotechnics in the African environment* (Vol. 1, pp. 99-104). Rotterdam: A.A. Balkema.

Monroy, R., Zdravković, L., & Ridley, A.M. (2015). Mechanical behaviour of unsaturated expansive clay under K0 conditions. *Engineering Geology*, 197, 112-131. http://doi.org/10.1016/j.enggeo.2015.08.006.

Murison, R.A., Gaspar, T.A.V., Heymann, G., Jacobsz, S.W., & Narainsamy, Y. (2024). Geotechnical investigation of a fissured highly expansive clay profile. In *Proceedings of the 7th International Conference on Geotechnical and Geophysical Site Characterization* (pp. 533-540), Barcelona. Barcelona. CIMNE. http://doi.org/10.23967/isc.2024.063.

Murison, R.A., Jacobsz, S.W., Gaspar, T.A.V., da Silva Burke, T.S. & Osman, A.S. (2023). Drying and wetting soil-water retention behaviour of a highly expansive clay under varying initial density. *E3S Web of Conferences*, 382, 09005. http://doi.org/10.1051/e3sconf/202338209005.

Murison, R.A., Jacobsz, S.W., da Silva Burke, T.S., Gaspar, T.A.V., & Osman, A.S. (2022). Monitoring bending moment distributions in large-scale laterally loaded piles using fibre Bragg gratings and vibrating wire strain gauges. In *Proceedings of the 10th International Conference on Physical Modelling in Geotechnics* (pp. 346-349), Daejoen, South Korea. Seoul: Korean Geotechnical Society.

Poulos, H.G. (1982). Single pile response to cyclic lateral load. *Journal of the Geotechnical Engineering Division*, 108(3), 355-375. http://doi.org/10.1061/AJGEB6.0001255.

SABS 920:2011. (2011). *Steel bars for reinforcement*. South African Bureau of Standards, Pretoria.

Skempton, A.W. (1953). The colloidal “activity” of clays. In *Proceedings of the 3rd International Conference on Soil Mechanics and Foundation Engineering* (Vol. 1, pp. 57-61), Zürich. Zürich: Swiss Society for SMFE.

van der Merwe, D.H. (1975). Plasticity index and percentage clay fraction of soils – in Speciality session B: Current theory and practice in building on expansive clays. In *Proceedings of the 6th African Regional Conference on Soil Mechanics and Foundation Engineering* (Vol. 2, pp. 166-167), Durban. Cape Town: A.A. Balkema.

Weston, D.J. (1980). Expansive roadbed treatment for Southern Africa. In *Proceedings of the 4th International Conference on Expansive Soils* (Vol. 1, pp. 339-360), Denver. Reston: ASCE.